SINTEF

SINTEF Energi AS
SINTEF Energy Research
Address:
Postboks 4761 Sluppen
NO-7465 Trondheim
NORWAY

Switchboard: +47 73597200

energy.research@sintef.no
www.sintef.no/energi
Enterprise /VAT No:
NO 939 350 675 MVA

Project memo

Reduction of Aerodynamic States in the STAS Wind Turbine Module

VERSION	**DATE**
1.0	2016-12-13

AUTHOR(S)
Karl O. Merz

CLIENT(S)	**CLIENTS REF.**
NOWITECH	

PROJECT NO.	**NO. OF PAGES AND APPENDICES:**
12X650	14

ABSTRACT
Two methods are examined for reducing the number of aerodynamic states in the wind turbine module of the STAS program. One method slaves the aerodynamic states to the blade structural modes, and the other method uses splines to represent the trends in the states as a function of radius. The two methods are shown to give practically equivalent results, significantly reducing the number of states in the model. Both methods have been implemented in the STAS wind turbine module.

PREPARED BY	**SIGNATURE**
Karl O. Merz	
APPROVED BY	**SIGNATURE**
Harald G. Svendsen	
PROJECT MEMO NO.	**CLASSIFICATION**
AN 16.12.70	Unrestricted

Document history

VERSION	DATE	VERSION DESCRIPTION
1.0	2016-12-13	Original document

SINTEF

Table of contents

1 Motivation

When the number of states in a model is large, the solution becomes more challenging, in terms of both time and numerical precision. The STAS wind power plant analysis program employs modal reduction in order to diagonalize the system matrices. The motivation is the ability to study pieces of the system behavior, such as control functions, in terms of a small number of modes. In addition, diagonalizing shortens, by two orders of magnitude, the calculation time for transfer functions. However, numerical problems have been observed in certain instances.[1] In particular, certain control filters, when active, can trigger inaccurate estimates of the rotor body rotation degree-of-freedom in the eigenvectors. The values can be checked by comparing transfer functions obtained with a full model,

$$\frac{\partial \mathbf{x}}{\partial \mathbf{u}} = (i\omega \mathbf{L} - \mathbf{A})^{-1}\mathbf{B} \qquad (1)$$

with those obtained after a modal reduction,

$$\frac{\partial \mathbf{x}}{\partial \mathbf{u}} = \mathbf{\Phi}(i\omega \mathbf{I} - \mathbf{\Lambda})^{-1}\mathbf{\Phi}^{-1}\mathbf{L}^{-1}\mathbf{B}. \qquad (2)$$

Inaccuracies in relevant parts of the eigenvectors $\mathbf{\Phi}$ will be seen as a mismatch in the computed $\partial \mathbf{x}/\partial \mathbf{u}$ transfer functions. This particular problem can be solved by eliminating the pure integrators in the model, such as the rotor azimuth, and balancing the system matrices before calculating the eigenvectors. Nonetheless, numerical precision is a concern, as the number of states will increase in proportion to the number of turbines in the wind power plant.

In order to improve the numerical conditioning of the eigenvectors, and obtain further increases in the speed of calculation, it is desired to reduce the number of states in the wind turbine model. The structural states are reduced in a straightforward manner, by computing the modes of each body (tower, nacelle, driveshaft, three blades) and retaining those of lowest natural frequency. This does not work for the aerodynamic states, which are largely independent of each other: the eigenvectors are often dominated by an individual element's states, rather than a meaningful distribution along the blade. No reduction is achieved.

Sønderby (2013) has addressed the issue of aerodynamic state reduction in some depth. Two classes of methods are proposed. In the first class of methods, modal reduction (at the system level) is performed prior to truncating the states; truncation is then performed either heuristically or by a formal balancing procedure. We set aside this class of methods, as it is the step of modal reduction that causes the observed numerical problems.[2] The second class of methods involves expanding the aerodynamic degrees-of-freedom in terms of some group of basis functions. For a given set of basis functions, states are mapped to generalized coordinates by $\mathbf{x} = \mathbf{\Psi}\mathbf{q}$, and the equations of motion can then be reduced as

$$\mathbf{\Psi}^T\mathbf{L}\mathbf{\Psi}\frac{d\mathbf{q}}{dt} = \mathbf{\Psi}^T\mathbf{A}\mathbf{\Psi}\mathbf{q} + \mathbf{\Psi}^T\mathbf{B}\mathbf{u}. \qquad (3)$$

Sønderby suggests that the basis functions may be chosen to be the (body) mode shapes of the blades.

The choice of blade mode shapes as basis functions means that the outboard portion of the blades is given preference, as it is here that the significant deformation – the weight in the basis

---

[1] This is not surprising: Moler and Van Loan (2003). They even name as "naïve" the use of eigenvectors in the equivalent time-domain operation of computing the matrix exponential. Yet, apart from a purely computational perspective, the use of eigenvectors is emphatically *not* naïve. The eigenvectors, together with the eigenvalues, tell us how the system responds, in a way which is straightforward for a human to interpret. They provide *insight*. And since we are computing them anyway, for insight, we might as well use them in further computations.

[2] Sønderby identifies other ways of approaching balanced truncation, such as frequency weighting, which do not require modal reduction upfront. Such an approach remains as a candidate method.

PROJECT NO.
12X650

PROJECT MEMO NO.
AN 16.12.70

VERSION
1.0

4 of 14

function – occurs. This problem can be avoided by static residualization (Sønderby 2013, pp 82-83), but only if one begins with a complete structural model of the blade. If the starting point is a truncated number of blade modes, then the use of these modes as basis functions will underestimate fluctuations in the aerodynamic states along the inner portions of the blades.

For most purposes, the inboard aerodynamic states are not in themselves of primary importance. Sønderby finds that the aeroelastic properties of a wind turbine are nicely predicted by slaving the aerodynamic to the structural modes; and we find the same here. On the other hand, there are niche cases where one wishes to know the aerodynamic states. An example could be a control system that incorporates, say, a local measure of the windspeed or angle-of-attack as an input. In this case the inboard aerodynamic transients might have an important influence on the closed-loop response.

If we consider the aerodynamic states to be independent from element to element along the blade, which is consistent with the blade element momentum (BEM) method of aerodynamic analysis,[3] then we need to choose basis functions which can represent an arbitrary profile extending from the root to the tip, including a uniform offset. At the same time, it is reasonable, based on typical blade designs and physical principles, to assume that the aerodynamic states will vary in a smooth manner along the blade. There are a variety of basis functions that fit these criteria. Here we propose and explore the use of spline curve segments.

2 Method

The idea is to represent, as a sequence of splines, the distribution of some aerodynamic state along the blade. Figure 1 shows a generic case; the profile might represent, say, the transient axial induced velocity. There are N aerodynamic elements along the blade, each of which has a coordinate r and a value x of the given type of state. These values likely form a smooth profile. To represent this profile in a reduced number of degrees-of-freedom, we can define splines based upon $M < N$ control points $\hat{r}$. The nice thing about this implementation of splines is that the control points relate directly to the values of the states. If we know the reduced, or generalized, coordinates $(\hat{r}, \hat{x})$ it is easy to visualize the intermediate values (r, x). Contrast this with some of the alternatives (Chebyshev polynomials, trigonometric functions) which result in more complicated relationships between the generalized coordinates and x values.

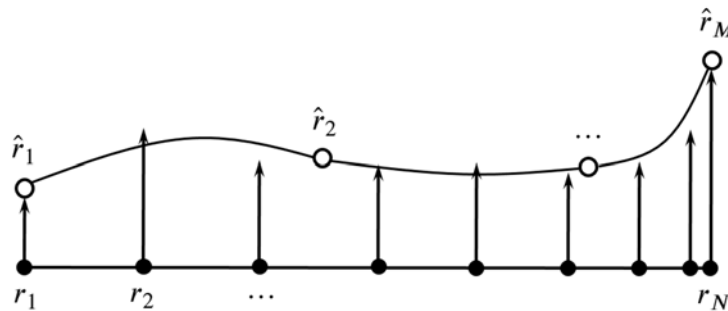Figure 1: A sketch representing some splines, whose shape is determined by the control points $(\hat{r}, \hat{y})$, fit approximately through a series of points (r, y).

A spline can be defined according to

$$x(r) = k_0 + k_1 s + k_2 s^2 + k_3 s^3, \tag{4}$$

where

---

[3] That is, the aerodynamic theory assumes radial independence of the control volumes for which momentum balance is performed.

PROJECT NO.
12X650

PROJECT MEMO NO.
AN 16.12.70

VERSION
1.0

5 of 14

$$s(r) := \frac{r - \hat{r}_i}{\hat{r}_{i+1} - \hat{r}_i}, \qquad 0 \le s \le 1, \qquad i = \{1, 2, \dots, M-1\}. \tag{5}$$

Given the control points $\hat{\mathbf{r}} := \left[\hat{r}_1, \hat{r}_2, \dots, \hat{r}_M\right]^T$, the coefficients of each spline segment can be determined by solving a linear matrix equation representing the boundary conditions: the spline must match $x(\hat{r}_i)$ and $x(\hat{r}_{i+1})$, and the first and second derivatives must be continuous across interior control points. At the exterior control points $\hat{r}_1$ and $\hat{r}_M$, the conditions

$$\frac{d^2 x}{dr^2}(\hat{r}_1) = \frac{1}{2} \frac{d^2 x}{dr^2}(\hat{r}_2) \qquad \text{and} \qquad \frac{d^2 x}{dr^2}(\hat{r}_M) = \frac{1}{2} \frac{d^2 x}{dr^2}(\hat{r}_{M-1}) \tag{6}$$

are selected, based on Hamming (1973). In a straightforward manner, the above boundary conditions can be written in the matrix form

$$\mathbf{F}(\hat{\mathbf{r}}) \, \mathbf{k} = \mathbf{G}(\hat{\mathbf{r}}) \, \hat{\mathbf{x}}, \tag{7}$$

which can be solved for $\mathbf{k}$. (Rather, we don't know particular values for $\hat{\mathbf{x}}$; it is the matrix $\mathbf{F}^{-1}\mathbf{G}$ that is sought.)

The next step is to interpolate the values $\mathbf{y}$ on the spline curves at the points $\mathbf{r}$. For a single value of (r, x) this is simply

$$x(r) = \begin{bmatrix} \dots & 1 & s & s^2 & s^3 & \dots \end{bmatrix} \begin{bmatrix} \vdots \\ k_0 \\ k_1 \\ k_2 \\ k_3 \\ \vdots \end{bmatrix} \tag{8}$$

where the placement along the $\mathbf{k}$ vector depends on which spline segment contains the given r coordinate.[4] For multiple points,

$$\mathbf{x}(\mathbf{r}) = \mathbf{S}(\mathbf{r}) \, \mathbf{k} = \mathbf{S}(\mathbf{r}) \, \mathbf{F}^{-1}(\hat{\mathbf{r}}) \, \mathbf{G}(\hat{\mathbf{r}}) \, \hat{\mathbf{x}} = \mathbf{H}\hat{\mathbf{x}}, \qquad \mathbf{H} := \mathbf{S} \, \mathbf{F}^{-1}\mathbf{G}. \tag{9}$$

With (9), we have obtained a linear mapping (for constant $\mathbf{r}$ and $\hat{\mathbf{r}}$) between the values $\hat{\mathbf{x}}$ at the control points and $\mathbf{x}$ at the elements.

The linear mapping (9) is used to transform, and reduce, the state equations. For a given set of aerodynamic states, these become at first

$$\mathbf{LH}\frac{d\hat{\mathbf{x}}}{dt} = \mathbf{AH}\hat{\mathbf{x}} + \mathbf{Bu}, \tag{10}$$

which is an overdetermined set of equations, as there are N rows but only M unknowns $\hat{\mathbf{x}}$. Equation (10) is solved in a least-squares sense as

$$\mathbf{H}^T \mathbf{LH}\frac{d\hat{\mathbf{x}}}{dt} = \mathbf{H}^T \mathbf{AH}\hat{\mathbf{x}} + \mathbf{H}^T \mathbf{Bu}. \tag{11}$$

In the actual implementation, (11), associated with a set of aerodynamic states, is but part of a much larger state space; but the global operation is accomplished in the form of (3) by placing $\mathbf{H}$ into $\mathbf{\Psi}$, if necessary padding with the identity matrix. Alternatively, the reduction of both aerodynamic and structural states can be combined into the operation (3), by forming $\mathbf{\Psi}$ blockwise, as appropriate, with the structural mode shapes and aerodynamic basis functions; see Eq. (17).

---

[4] This, together with (4), is computationally not the most efficient way to represent a spline, but it is easy to work with, and the overhead in the context of the STAS program is negligible.

3 Illustrative Results

It is instructive to begin with an elemental case, one which includes the important features of the problem, but in their most elementary form. Afterwards, some results from the STAS program are demonstrated.

3.1 An elemental case

We consider a series of carts connected by springs, as sketched in Fig. 2. The position of the ith cart relative to equilibrium is r_i, its mass is m_i, and it is coupled to the previous cart with a spring of stiffness k_i. A force $\bar{F}_i$ acts on the cart, which is related to an input force F_i through a low-pass filter, containing also a component of damping, as

$$\frac{d\bar{F}_i}{dt} = -\alpha_i \bar{F}_i + \alpha_i \left(F_i - c_i \frac{dr_i}{dt} \right). \tag{12}$$

The mass-spring system could be the blade flapwise flexibility, and the force is then representative of the aerodynamic lift, with (12) being a transient aerodynamic effect like circulation lag.
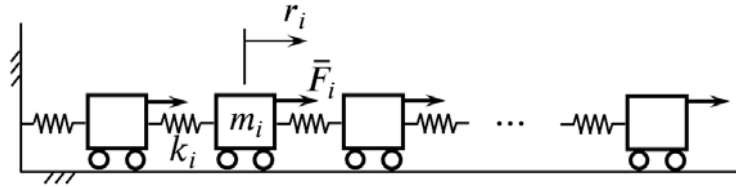

Figure 2: A mass-spring representation of blade deflection.

Assembling the r_i, $\dot{r}_i$, and $\bar{F}_i$ states into vectors, the state matrices look like this:

$$\begin{bmatrix} \mathbf{I} & \mathbf{0} & \mathbf{0} \\ \mathbf{0} & \mathbf{M} & \mathbf{0} \\ \mathbf{0} & \mathbf{0} & \mathbf{I} \end{bmatrix} \frac{d}{dt} \begin{bmatrix} \mathbf{r} \\ \dot{\mathbf{r}} \\ \mathbf{F} \end{bmatrix} = \begin{bmatrix} \mathbf{0} & \mathbf{I} & \mathbf{0} \\ -\mathbf{K} & \mathbf{0} & \mathbf{I} \\ \mathbf{0} & -\mathbf{C}_\alpha & -\mathbf{A}_\alpha \end{bmatrix} \begin{bmatrix} \mathbf{r} \\ \dot{\mathbf{r}} \\ \mathbf{F} \end{bmatrix} + \begin{bmatrix} \mathbf{0} \\ \mathbf{0} \\ \mathbf{A}_\alpha \end{bmatrix} \mathbf{F}. \tag{13}$$

$\mathbf{M}$ is a diagonal mass matrix, $\mathbf{K}$ is a standard, symmetric stiffness matrix, $\mathbf{C}_\alpha$ contains the product of $\alpha_i c_i$ along the diagonal, and $\mathbf{A}_\alpha$ contains α_i along the diagonal. The state equations (13) are subsequently reduced as in (11).

We now examine how well different basis functions predict the structural and aerodynamic response. For this purpose, the model of Fig. 2 is given parameters that represent a generic wind turbine blade. Let there be ten mass-spring carts, or rather ten uniformly-spaced elements along the blade. Indexing from the root to the tip, the masses are set to

$$\mathbf{m} = \text{diag}(\mathbf{M}) = [10 \quad 9 \quad \dots \quad 1]^T,$$

stiffnesses to

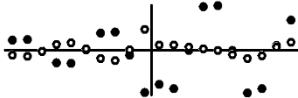$$\mathbf{k} = [1000 \quad 900 \quad \dots \quad 100]^T,$$

(aerodynamic) damping to
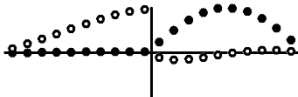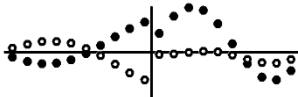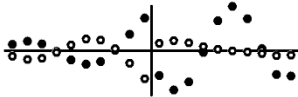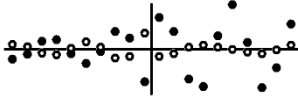
$$c_i = 2\zeta \sqrt{k_i m_i}, \qquad \zeta = 0.1,$$

and low-pass filter time constants to

$$\boldsymbol{\alpha} = \text{diag}(\mathbf{A}_\alpha) = 2\pi \, [0.5 \quad 0.6 \quad \dots \quad 1.4]^T \ \text{rad/s}.$$

The units are unimportant, apart from time, as we will be referring to frequencies in Hz.

PROJECT NO.
12X650

PROJECT MEMO NO.
AN 16.12.70

VERSION
1.0

7 of 14

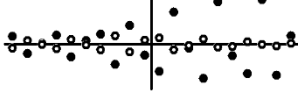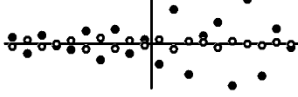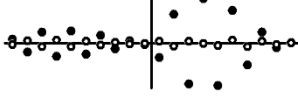Table I: A list of modes associated with the spring-mass model, using the example set of parameters. Oscillatory modes are indicated by a natural frequency and damping ratio, while the value of the root is given for purely decaying modes. Mode shapes are sketched, with black points indicating real and white points imaginary values. "Real" and "imaginary" is not important, only the relative phase. Structural states are shown at left, and aerodynamic states at right.

Struct. mode	f_n (Hz)	ζ	Shape: structural | aerodynamic
1	0.385	0.459	
2	0.835	0.116	
3	1.229	0.051	
4	1.597	0.028	
5	1.936	0.017	
6	2.243	0.012	
7	2.510	0.008	
8	2.736	0.007	
9	2.917	0.005	
10	3.053	0.003	

PROJECT NO.
12X650

PROJECT MEMO NO.
AN 16.12.70

VERSION
1.0

8 of 14

Aero. mode	s (s^{-1})	
11	-2.830	
12	-3.249	
13	-3.824	
14	-4.406	
15	-4.986	
16	-5.565	
17	-6.147	
18	-6.736	
19	-7.344	
20	-7.986	

PROJECT NO.
12X650

PROJECT MEMO NO.
AN 16.12.70

VERSION
1.0

9 of 14
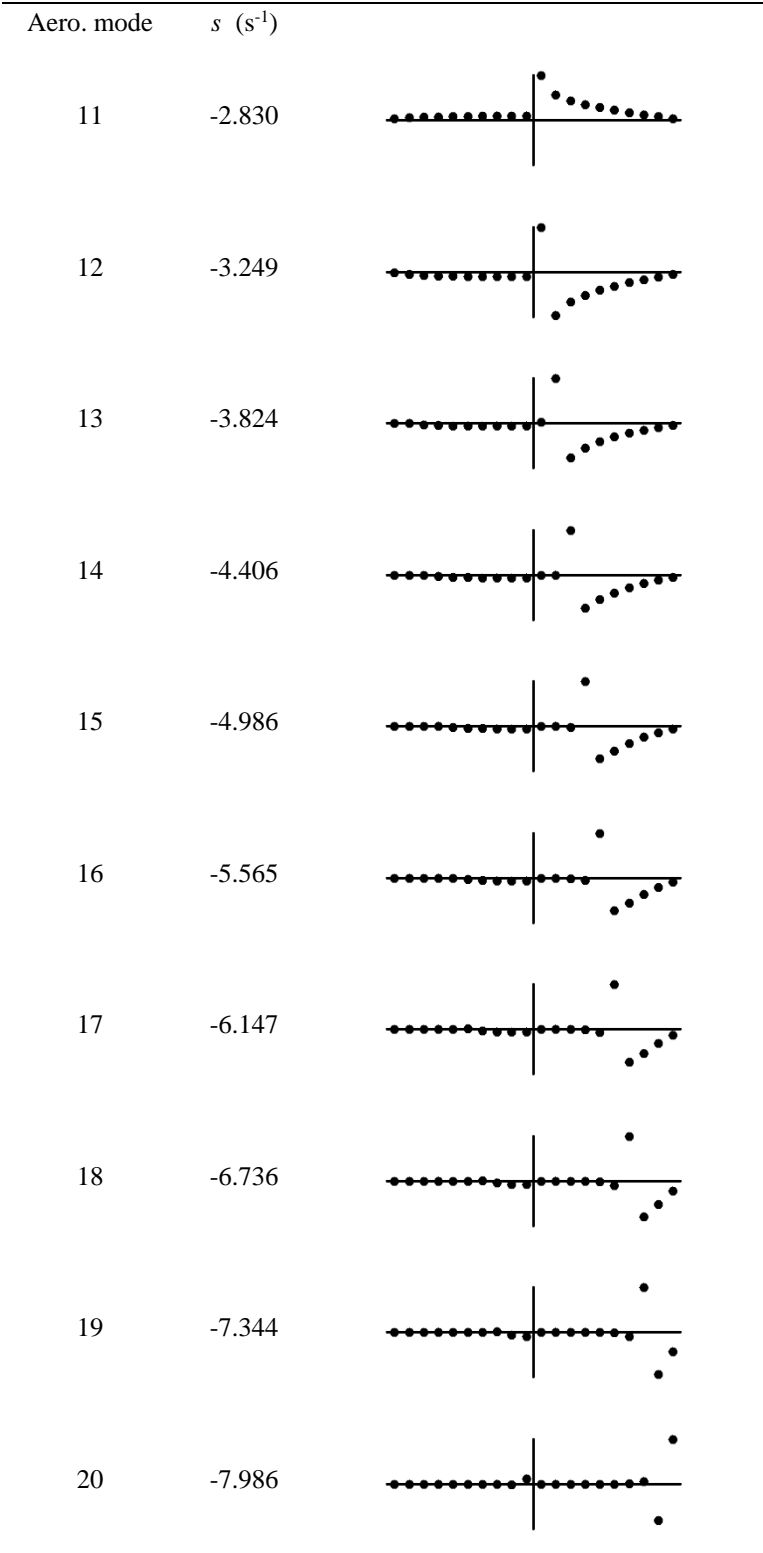
With this setup, the modes of the full model are listed in Table I. There is a set of oscillatory structural modes which are coupled to aerodynamic states, the latter providing damping, especially at low frequencies. Then there is a set of overdamped (purely decaying) aerodynamic modes, associated with the low-pass filtering of the aerodynamic states. These modes are not coupled significantly with structural motions. The aerodynamic modes also exhibit discontinuities, a feature which arises due to the assumption that adjacent BEM control volumes, and the associated aerodynamic elements, are independent.

Before proceeding with the modal calculations for reduced models, let us take a quick look at the use of splines to represent the aerodynamic states. The input is some pattern of force $\mathbf{F}$ along the blade. Say that the distribution of fluctuating forces is

$$\mathbf{F} = \gamma(t)\,\mathbf{F}_0, \quad \mathbf{F}_0 = [0.3\ 0.5\ 0.6\ 0.7\ 0.8\ 0.9\ 1.0\ 1.0\ 0.8\ 0.4], \tag{14}$$

representing in a very rough manner the expected pattern of circulatory loading.[5] The distribution of the filtered forces $\overline{\mathbf{F}}$ will be a function of frequency, as the filter frequencies α_i vary along the blade. We consider a model consisting only of the aerodynamic states,

$$\frac{d\overline{\mathbf{F}}}{dt} = -\mathbf{A}_\alpha \overline{\mathbf{F}} + \mathbf{A}_\alpha \mathbf{F}, \tag{15}$$

with spline reduction according to (9) and (11). Spline control points are set to elements 1, 4, 8, and 10 along the blade. The results for the transfer function $\partial\overline{\mathbf{F}}/\partial\gamma$, $\gamma(t)$ being the scale factor on the load pattern, are shown in Fig. 3. In this case, four splines provide a reasonable representation of the load pattern, including the trends with frequency. A more accurate fit could be obtained by using additional splines, and a coarser fit with fewer splines.
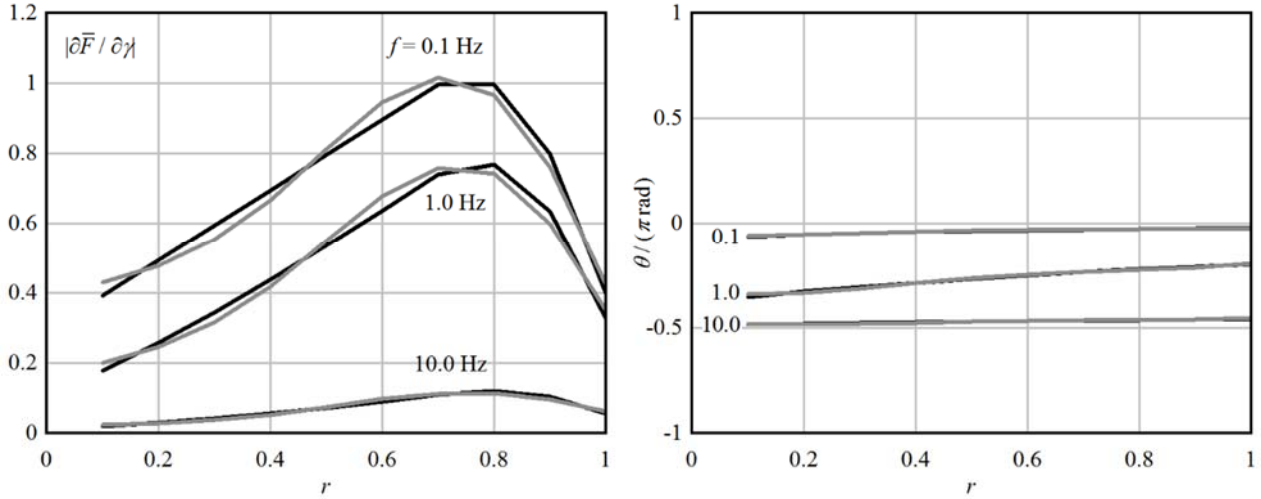

Figure 3: An example of spline fits to a pattern reminiscent of the loading along a blade. At left: magnitude, at right: phase. Black curves show the assumed load profile (14), and gray curves the values at the same radial locations, obtained using splines.

Seeking to reduce the size of the full aeroelastic model (13), we apply a modal reduction to the structural states. This takes the form of an eigenvalue problem,

---

[5] This is just for illustration. In the actual wind turbine model the aerodynamic states represent angles-of-attack, induced velocities, and the like, not directly forces, so there is no reason to be too picky about the accuracy of our "force" distribution. For instance, we could have said that the aerodynamic input was induced velocity and chosen a distribution of 0.33 along the central part of the blade, increasing sharply near the root and tip. The key point is that dramatic things happen near the root and especially the tip.

$$\left(\omega^2 \mathbf{M} - \mathbf{K}\right)\mathbf{r} = \mathbf{0}. \tag{16}$$

That is, we solve for the body modes of the structure, without any aerodynamics. Sorting in terms of natural frequency, let the first n out of the N mode shapes so obtained be stored in the shape matrix $\mathbf{\Phi}$, such that $\mathbf{r} \approx \mathbf{\Phi q}$, up to the vicinity of the nth natural frequency. For demonstration, we take $n = 4$. The resulting mode shapes look similar to those of the structural modes 1 through 4 in Table I.

The two models to be compared are both based on (13) and reduced according to (11). Both also employ modal reduction of the structural states, using $\mathbf{\Phi}$. The difference is in the part of the $\mathbf{\Psi}$ matrix associated with the aerodynamic states:

$$\mathbf{\Psi} = \begin{bmatrix} \mathbf{\Phi} & \mathbf{0} & \mathbf{0} \\ \mathbf{0} & \mathbf{\Phi} & \mathbf{0} \\ \mathbf{0} & \mathbf{0} & \mathbf{\Phi} \end{bmatrix} \quad \text{or} \quad \mathbf{\Psi} = \begin{bmatrix} \mathbf{\Phi} & \mathbf{0} & \mathbf{0} \\ \mathbf{0} & \mathbf{\Phi} & \mathbf{0} \\ \mathbf{0} & \mathbf{0} & \mathbf{H} \end{bmatrix}, \tag{17}$$

where the former slaves the aerodynamic to the structural states, and the latter employs splines.

Table II compares the modal properties of the first four modes of Table I. A reduction of the aerodynamics based on structural modes provides, as expected, an excellent prediction of the aeroelastic structural modes. Splines are good, but less efficient: it would take additional spline degrees-of-freedom to match the accuracy of four structural modes.

Table II: A comparison of structural modes

Mode ID	Full model		Slaved to structural modes		Splines	
	f_n	ζ	f_n	ζ	f_n	ζ
1	0.385	0.459	0.385	0.459	0.385	0.459
2	0.835	0.115	0.835	0.116	0.835	0.116
3	1.229	0.051	1.229	0.051	1.216	0.045
4	1.597	0.028	1.594	0.029	1.583	0.022

Figure 4 shows transfer functions from γ – retaining the force distribution of (14) – to the position r and filtered force $\bar{F}$ at the root element, and the first element inboard of the tip. The structural mode basis is marginally better at capturing the influence of the aerodynamic forces on structural displacements, as seen in the upper plots at the high end of the frequency range. In the lower plots, it is evident that structural modes do not resolve the fluctuations in aerodynamic states near the root. The discrepancy disappears beyond the corner frequency of the low-pass filter, 0.5 Hz at the root.

This investigation of an elementary model has confirmed Sønderby's result that the aerodynamic states may be slaved to the structural modes of the blade. It has also been shown that splines can be used for the same purpose, though they are somewhat less efficient, in terms of the accuracy for a given number of degrees-of-freedom. An advantage of splines is that they are more naturally able to match the aerodynamics at the blade root. There is no single correct approach; other basis functions could also be employed.
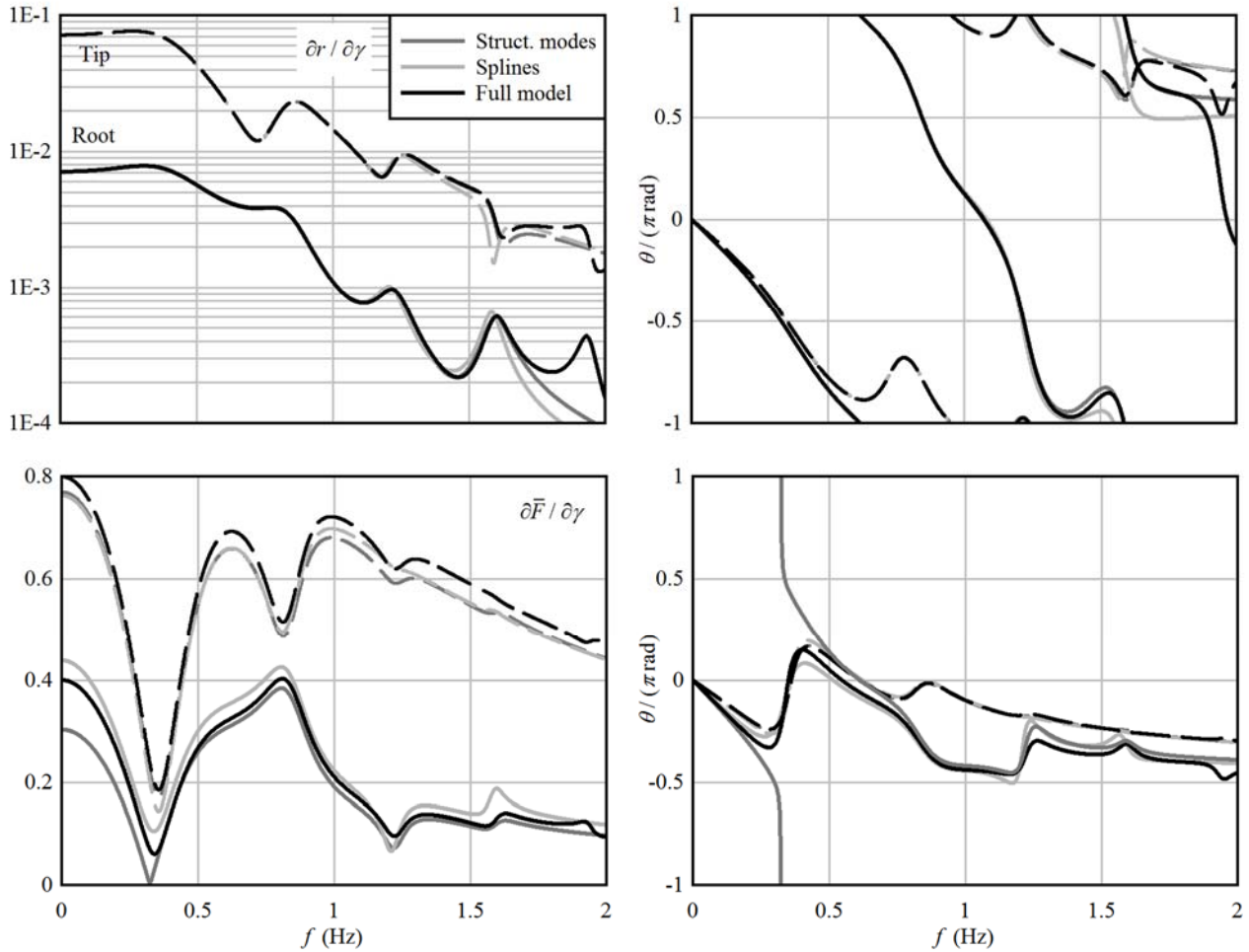
PROJECT NO.
12X650

PROJECT MEMO NO.
AN 16.12.70

VERSION
1.0

11 of 14

Figure 4: Transfer functions from the scale factor γ to the position (top) and aerodynamic (bottom) states, at the root and tip elements.

3.2 Implementation in the STAS program

Both versions of (17) are implemented in the wind turbine module of the STAS program. We illustrate the results with a case study of a 10 MW wind turbine (Bak *et al*. 2013) operating in a 16 m/s wind. The full model consists of sixteen elements along the blade ($r/R = 0.06, 0.11, 0.17, 0.24, 0.31,$ $0.39, 0.46, 0.54, 0.62, 0.69, 0.76, 0.82, 0.88, 0.92, 0.96, 0.99$), serving as both aerodynamic and structural elements. The reduced models consist of respectively the first six blade flapwise modes, and six spline control points.

Figure 5 shows the transfer functions from the rotor-average windspeed to the lift force at selected locations along the blade. These are loosely analogous to the plots at the bottom of Fig. 4, although the dynamics of a wind turbine are more complicated than the elementary case of Section 3.1.

In Fig. 5, the low-frequency asymptote of the curves corresponds to the change in the steady-state operating point of the wind turbine under a perturbation in the windspeed. Consistent with the negative slope in the thrust curve above the rated windspeed, the change in lift opposes the windspeed, over the outer part of the blade. This is due to the control of the blade pitch angle, to maintain the rated speed and power. The inboard element does not behave as a typical airfoil, and here the lift is in-phase with the windspeed, despite the change in pitch.

The control of rotor speed results in a peak in the pitch response, and thus the lift force, at a frequency of just over 0.1 Hz. There is a zero in the transfer function in the vicinity of the first tower

PROJECT NO.
12X650

PROJECT MEMO NO.
AN 16.12.70

VERSION
1.0

12 of 14

resonant frequency, about 0.24 Hz. This is related to the wind-driven fore-aft motion of the tower, which when in-phase with the windspeed, ends up cancelling most of the relative velocity (Merz 2016).

It is evident from Fig. 5 that a slightly better prediction of the loads is obtained with splines. This is consistent with the results of the elementary mass-spring-force model of the previous section. Table III lists the natural frequency and damping ratio of a selection of aeroelastic modes, which together represent the rotor and tower dynamics up to 1 Hz. There is no meaningful difference between the full model and the two reduced models, apart from the beneficial reduction in the number of degrees-of-freedom.
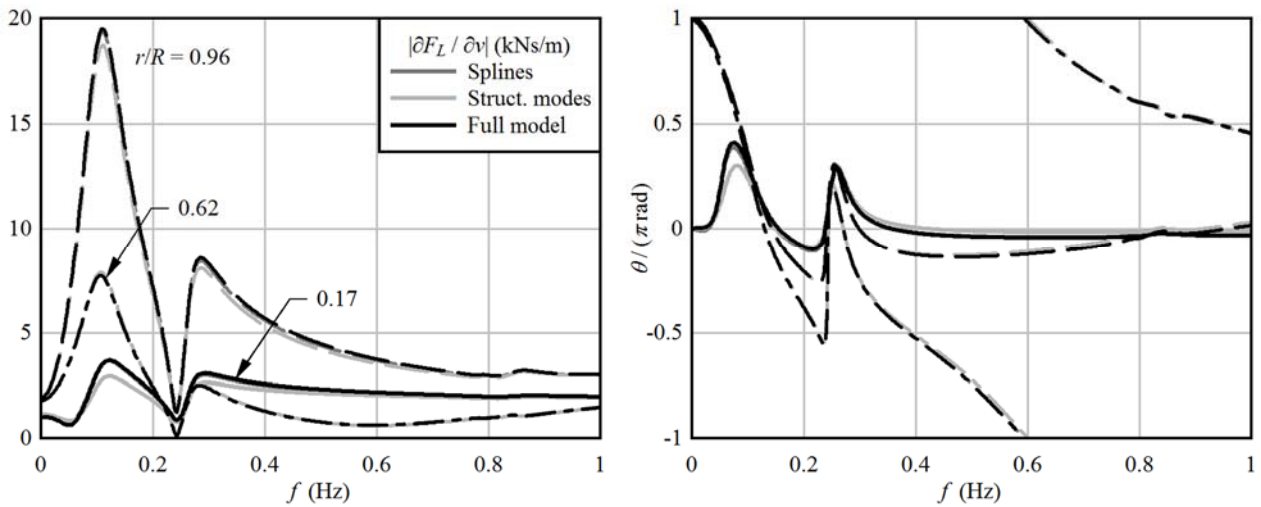

Figure 5: Transfer functions between rotor-average axial windspeed and the lift force on blade elements at three radial locations.

Table III: Comparison of modal reduction techniques on a selection of modes of the wind turbine system, including aeroelastic, electrical, and control dynamics. A full controller is employed, including active damping of the tower.

Mode	Full model		Slaved to struct. modes		Splines	
N_{DOF}	504		297		297	
	f_n	ζ	f_n	ζ	f_n	ζ
Rotor speed control	0.103	0.349	0.104	0.346	0.103	0.348
Tower side-to-side	0.239	0.044	0.239	0.044	0.239	0.044
Tower fore-aft	0.259	0.089	0.259	0.090	0.259	0.089
Rotor whirling 1	0.313	0.608	0.313	0.609	0.313	0.608
Rotor whirling 2	0.499	0.734	0.500	0.734	0.500	0.734
Rotor whirling 3	0.569	0.676	0.567	0.677	0.567	0.677
Collective blade flap	0.748	0.715	0.747	0.715	0.748	0.715
Edgewise whirling/tower	0.786	0.018	0.786	0.018	0.786	0.018
Second tower SS/FA	0.830	0.026	0.830	0.026	0.830	0.026
Rotor whirling 4	0.840	0.847	0.843	0.845	0.843	0.846
Second tower FA/SS	0.850	0.031	0.850	0.031	0.850	0.031

PROJECT NO.
12X650

PROJECT MEMO NO.
AN 16.12.70

VERSION
1.0

13 of 14

4 Conclusions

Two methods for reducing the number of aerodynamic states have been implemented in the STAS wind power plant analysis program. One method, recommended by Sønderby (2013), slaves the aerodynamic states to the structural modes of the blades. The other approach uses splines, which in effect fit a smooth profile, as a function of radius, to the aerodynamic states associated with the blade elements. The two methods of model reduction are shown to give essentially equivalent results. To the very small degree by which they are distinguishable, the spline approach gives a better estimate of the aerodynamic loads, while the modal approach gives a better estimate of the aeroelastic response.

5 References

Bak C, *et al*. (2013). *Description of the DTU 10 MW Reference Wind Turbine*. DTU Wind Energy Report-I-0092, Technical University of Denmark.

Hamming RW (1973). *Numerical Methods for Scientists and Engineers*. New York, McGraw-Hill, Inc.

Merz KO (2016). Basic control tuning for large offshore wind turbines. Wind Energy Science 1, 153-175.

Moler C, Van Loan C (2003). Nineteen dubious ways to compute the exponential of a matrix, twenty-five years later. *SIAM Review* 45, 3-49.

Sønderby IB (2013). *Low-order aeroelastic models of wind turbines for controller design*. PhD Thesis, Department of Wind Energy, Technical University of Denmark.